REPORT DOCUMENTATION PAGE

Form Approved OMB NO. 0704-0188

1. REPORT DATE (DD-MM-YYYY)	2. REPORT TYPE	3. DATES COVERED (From - To)
22-09-2021	Final Report	1-Oct-2017 - 30-Apr-2021

4. TITLE AND SUBTITLE
Final Report: Voltage Control of Magnetism in THz Regime via Magnon-Phonon Coupling

5a. CONTRACT NUMBER
W911NF-17-1-0364

5b. GRANT NUMBER

5c. PROGRAM ELEMENT NUMBER
611102

6. AUTHORS

5d. PROJECT NUMBER

5e. TASK NUMBER

5f. WORK UNIT NUMBER

7. PERFORMING ORGANIZATION NAMES AND ADDRESSES
University of California - Los Angeles
Office of Contract and Grant Administration
11000 Kinross Avenue, Suite 211
Los Angeles, CA 90095 -1406

8. PERFORMING ORGANIZATION REPORT NUMBER

9. SPONSORING/MONITORING AGENCY NAME(S) AND ADDRESS (ES)
U.S. Army Research Office
P.O. Box 12211
Research Triangle Park, NC 27709-2211

10. SPONSOR/MONITOR'S ACRONYM(S)
ARO

11. SPONSOR/MONITOR'S REPORT NUMBER(S)
71598-EL.7

12. DISTRIBUTION AVAILIBILITY STATEMENT
Approved for public release; distribution is unlimited.

13. SUPPLEMENTARY NOTES
The views, opinions and/or findings contained in this report are those of the author(s) and should not contrued as an official Department of the Army position, policy or decision, unless so designated by other documentation.

14. ABSTRACT

15. SUBJECT TERMS

16. SECURITY CLASSIFICATION OF:			17. LIMITATION OF ABSTRACT	15. NUMBER OF PAGES	19a. NAME OF RESPONSIBLE PERSON
a. REPORT	b. ABSTRACT	c. THIS PAGE			Gregory Carman
UU	UU	UU	UU		19b. TELEPHONE NUMBER 310-825-6030

RPPR Final Report
as of 01-Oct-2021

Agency Code: 21XD

Proposal Number: 71598EL **Agreement Number: W911NF-17-1-0364**
INVESTIGATOR(S):

Name: PhD Gregory P. Carman
Email: carman@seas.ucla.edu
Phone Number: 3108256030
Principal: Y

Organization: **University of California - Los Angeles**
Address: Office of Contract and Grant Administration, Los Angeles, CA 900951406
Country: USA
DUNS Number: 092530369 EIN: 956006143
Report Date: 31-Jul-2021 Date Received: 22-Sep-2021
Final Report for Period Beginning 01-Oct-2017 and Ending 30-Apr-2021
Title: Voltage Control of Magnetism in THz Regime via Magnon-Phonon Coupling
Begin Performance Period: 01-Oct-2017 **End Performance Period:** 30-Apr-2021
Report Term: 0-Other
Submitted By: PhD Gregory Carman Email: carman@seas.ucla.edu
Phone: (310) 825-6030

STEM Degrees: 1 **STEM Participants:**

Major Goals: The major aim of this work is to open a new pathway towards THz devices by demonstrating THz magnon-phonon coupling for the first time. To accomplish this, we have targeted antiferromagnets as a material class of interest because their resonance frequencies are much higher than ferromagnets and are often in the THz range. This fact indicates the existence of desirable THz magnon modes, but the level of phonon coupling with these modes is so far unknown. To address this question, our work under this contract seeks to investigate the fundamental physics of antiferromagnets in two main areas: 1) check whether magneto-mechanical coupling at THz is present, since definitive proof is generally lacking, and 2) to prove that strain can be used as a method to control antiferromagnetic states, since this would enable creation or control of THz frequency magnon/phonon excitation.

To prove these two key points, we aim to develop a series of test devices consisting of candidate magnetostrictive antiferromagnetic materials layered into composites with piezoelectric substrates. Using this approach, the composite's strain is tunable with voltage, and can be driven to oscillate at high frequency, thereby allowing observation of both the fundamental strain effects and injection of high frequency phonons. Design of these devices is proceeding following a 3-step process (see Figure 1 below) consisting of 1) sophisticated multiphysical modeling to predict device behavior, 2) fabrication of a device informed by the model results, and 3) testing both of the fundamental mechanical coupling and the device's frequency-dependent magnon-phonon coupling. The goal of this final testing phase is to identify the underlying physics of the mechanical coupling in antiferromagnets, and will require both table-top electrical testing and sophisticated probing of the magnetic properties at national lab beamlines.

To achieve these objectives we focus on two materials, both of which are reported to exhibit three key characteristics, antiferromagnetic order, magnetostriction, and magnetoresistance (magnetoresistance helps to identify the antiferromagnetic state). These two materials are NiO and the 50-50 composition of L10 ordered alloy FeMn.In addition to these materials, this research covers additional studies conducted by the researchers focusing on ferrimagnetic materials and their related magnetostriction as well as contributions from elemental magnetic moments. While these ferrimagnetic topics are not covered in detail within this report they are part of the published literature that this research supported, i.e. see dissemination section.

Understanding the complex dynamics of antiferromagnets and ferrimagnetics through modeling, fabrication and testing provides a clear path to explore fundamental physics in the context of new and interesting application spaces. Namely, the research conducted here will enable 1) new classes of THz electronic devices, 2) new computational methods verified with experiments, and 3) a fundamental understanding of dynamic THz

magnon/phonon interactions. This work aims to launch a major shift towards cheaper and faster electronic devices for future applications.

Please see upload document for complete Major Goals with figures.

Accomplishments: Over the course of this contract, significant progress was made towards the goal of demonstrating magnetoelectric control of antiferromagnetic states at THz frequencies. Below, the key sections (Modeling, Fabrication, and Testing) are overviewed with more details presented in the uploaded document section of this report.

Modeling Achievements

The primary goals of the modeling effort were to accurately predict device behavior in magnetostrictive antiferromagnet/piezoelectric composites with THz magnon-phonon coupling, and to support material characterization and testing. These goals were achieved through a combination of numerical and analytical modeling. Using a multiphysical finite element model in which the mechanics and magnetics of magnetostrictive antiferromagnets are fully coupled, the response of an antiferromagnetic bit to a time-dependent strain was simulated. This confirmed the expected THz-speed switching capability of antiferromagnets, as well as demonstrated that antiferromagnetic switching speed is limited by the material's mechanical wave speed. An example of how this finite element model may be used as a tool to guide device design was shown through simulation of a strain-programmable antiferromagnetic nanowire for neuromorphic computing applications. Finally, this model supported the testing thrust by providing the expected strain distribution in an antiferromagnetic hall bar/piezoelectric heterostructure. On the analytical side, the dependence of Spin Hall Magnetoresistance (SMR) signal on applied strain was calculated for polycrystalline samples and compared to testing results with good agreement, and a model relating antiferromagnetic susceptibility and spin-flop field to saturation magnetostriction was developed and used in measurement of FeMn saturation magnetostriction.

Fabrication Achievements

The goal of the fabrication effort was to deposit quality FeMn and NiO thin films, and to characterize their antiferromagnetic ordering. FeMn was successfully deposited via DC sputtering, while NiO was deposited using electron beam evaporation. Both materials were deposited on both Si and 500 micron-thick PMN-PT (piezoelectric) substrates. Using x-ray diffraction (XRD) and transmission electron microscopy's (TEM) scanning electron area diffraction (SEAD), the crystalline phase of each sample was determined. Following this, using the 6.3.1 beamline at Lawrence Berkely National Lab, both materials were characterized using x-ray magnetic linear dichroism (XMLD) and x-ray magnetic circular dichroism (XMCD). These measurements can directly probe the orientation of magnetic moment with atomic specificity, allowing one to determine both the orientation of the Neel vector in antiferromagnetic samples, as well as the element-wise contribution to magnetic moment. Using these measurements, the ferromagnetic to antiferromagnetic transition temperature for both FeMn and NiO was determined, and it was observed that Mn dominates the magnetic moment of FeMn, indicating the presence of L10 ordering which may be favorable for magnetostriction.

Testing Achievements

The primary goal of the testing effort was to enable measurement of the effect of strain on magnetostrictive antiferromagnets using table-top equipment. To this end, anisotropic magnetoresistance (AMR) was used to measure changes in the antiferromagnetic state of FeMN, while Spin Hall Magnetoresistance (SMR) was used to measure the same in NiO. For this measurement, FeMN and NiO films were deposited on Si and PMN-PT substrates and patterned into hall bar structures. Firstly, a baseline change in magnetoresistance due to a 90° switch of the antiferromagnetic state was measured by applying fields ranging from -11 to +11 Tesla. NiO showed a change in resistance of 0.007%, while FeMn showed a change in resistance of 0.0014%. Next, the effect of strain was determined by repeating the SMR measurements in the presence of applied strains ranging from 0 to 280 με. For NiO, the change in SMR signal due to applied strain was similar to that caused by a 3 T applied field and matched the expectation of negative magnetostriction in NiO. This result shows the significant influence of magnetoelastic energy on the antiferromagnetic state. Finally, the SMR measurement was repeated on polycrystalline NiO samples. Even with polycrystalline structure, the effect of strain on NiO's antiferromagnetic state was significant and demonstrated that a strain-induced spin-flop transition may be possible in the absence of applied field.

In addition to measuring the magnetoresistance changes in antiferromagnets due to strain, the effect of varying deposition process parameters on FeMn thin films was measured. By varying the argon working pressure between 5, 10, and 15 mTorr, the residual stresses in the FeMn thin film can be tuned. While the 5 mTorr sample showed paramagnetic response, both the 10 and 15 mTorr FeMn films showed antiferromagnetic response. By measuring the difference in susceptibility and spin flop field between the 10 and 15 mTorr samples, the saturation magnetostriction of FeMn was determined using the previously mentioned analytical model (λ_(s)=-141 ppm).

Training Opportunities: During the last year, the Ph.D. student, Paymon Shirazi, who is supported by the DoD Science Mathematics and Research for Transformation (SMART) scholarship spent approximately 3 months in a joint internship between the Naval Surface Center (NSWC) Corona Division, the National Institute of Science & Technology (NIST), and UCLA working on DoD relevant research at UCLA cleanroom facilities, where his research expenses were supported under this grant. During this period, he was mentored by two leading physicists (Randolph Elmquist & David Newell) in the physical measurement laboratory at NIST. The internship spawned into an on-going collaboration between the three institutions with the aim of fabricating devices employing our antiferromagnet thin film developments within their physical-standards devices relevant to both DoD and NIST research efforts. This research will be submitted as a joint journal publication in the near future.

RPPR Final Report
as of 01-Oct-2021

Results Dissemination: 1. "Strain control of the Neel vector in Mn-based antiferromagnets" By:Park, IJ (Park, In Jun) ; Lee, T (Lee, Taehwan); Das, P (Das, Protik) ; Debnath, B (Debnath, Bishwajit) ; Carman, GP (Carman, Greg P.); Lake, RK (Lake, Roger K.),APPLIED PHYSICS LETTERS, Volume: 114 Issue: 14. Article Number: 142403, DOI: 10.1063/1.5093701, Published: APR 8 2019

2."Voltage Control of Antiferromagnetic Phases at Near-Terahertz Frequencies" By:Barra, A (Barra, Anthony) ; Domann, J (Domann, John) ; Kim, KW (Kim, Ki Wook) ; Carman, G (Carman, Greg),PHYSICAL REVIEW APPLIED, Volume: 9 Issue: 3, Article Number: 034017, DOI: 10.1103/PhysRevApplied.9.034017Published: MAR 21 2018

3. “Effective Strain Manipulation of the Antiferromagnetic State of Polycrystalline NiO” By: Barra, A (Barra, Anthony) ; Ross, A (Ross, Andrew) ; Baldrati, L (Baldrati, Lorenzo) ; Lebrun, R (Lebrun, Romain) ; Chavez, A (Chavez, Andres), Shirazi, P (Shirazi, Paymon) ; Schneider, J (Schneider, Joseph Devin) ; Wang, Q (Wang, Qianchang) ; Carman, GP (Carman, Greg) ; Kläui, M (Kläui, Mathias), APPLIED PHYSICS LETTERS, Volume 118, Issue 17 (2021).

4. “Magnetic Memory with Antiferromagnets and Multilayers” By: Barra, A (Barra, Anthony), UCLA PH.D. DISSERTATION To be submitted: OCT 1 2019

5. “Novel Magnetoelastic Materials for Multiferroic Applications” By: Lee, T (Lee, Taehwan), UCLA PH.D. DISSERTATION Published: OCT 1 2019

6. “Rare-Earth Orbital Moment Contributions to the Magnetic Anisotropy in Magnetostrictive Tb0.3Dy0.7Fe2” By: Shirazi, P (Shirazi, Paymon) ; Lee, T (Lee, Taehwan) ; Panduraga, MK (Panduranga, Mohanchandra K.) ; N’Diaye, AT, (N’Diaye, Alpha T.) ; Barra, A (Barra, Anthony) ; Carman, GP (Carman, Greg P.), APPLIED PHYSICS LETTERS, Volume:118 Issue:16, Article Number: 162401, DOI: 10.1063/5.0049326, Published: MAR 31 2021

7. “Single magnetic domain Terfenol-D microstructures with passivating oxide layer” By: Panduranga, MK (Panduranga, Mohanchandra K.), Xiao, ZY (Xiao, Zhuyun), Schneider, JD (Schneider, Joseph D.), Lee, T (Lee, Taehwan), Klewe, C (Klewe, Christoph), Chopdekar, R (Chopdekar, Rajesh),Shafer, P (Shafer, Padraic), N'Diaye, AT (N'Diaye, Alpha T.), Arenholz, E (Arenholz, Elke),Candler, RN (Candler, Rob N.), Carman, GP (Carman, Gregory P.) JOURNAL OF MAGNETISM AND MAGNETIC MATERIALS, Volume 528, Article Number 167798, DOI: 10.1016/j.jmmm.2021.167798, Published: JUN 15, 2021

8. “Stress Induced Reorientation of the Neel Vector in Antiferromagnetic FeMn Thin Films” By:Shirazi, P (Shirazi, Paymon);Panduraga, MK (Panduranga, Mohanchandra K.); Barra,A(Barra, Anthony); Lee,T (Lee, Taehwan); Guevara, M (Guevara, Micheal) ; Carman, GP (Carman, Greg P.) TO BE SUBMITTED (APPLIED PHYSICS LETTERS)

9. “Magnetostrictive Ferri and Antiferromagnetic Thin Films for Multiferroic Applications” By: Shirazi, P (Shirazi, Paymon), UCLA PH.D. DISSERTATION To be submitted: Dec 1 2021

10. “Picosecond Strain Control of Antiferromagnetic States for Neuromorphic Computing” By: Nance, J., Roxy, K., Bhanja, S., Carman, GP. TO BE SUBMITTED (November 2021).

Honors and Awards: Greg Carman was appointed to the Ben Rich Lockheed Martin Chair in the Mechanical & Aerospace Engineering Department

Greg Carman has been asked to provide the plenary lecture at the joint MMM/Intermag conference 2022

Beamtime Awarded – Lawrence Berkeley National Laboratory (ID: ALS – 11320) for study of antiferromagnetic/ferrimagnetic materials

Protocol Activity Status:

Technology Transfer: see training section for potential interactions with DoD and Govt Labs

RPPR Final Report
as of 01-Oct-2021

PARTICIPANTS:

Participant Type: Graduate Student (research assistant)
Participant: John Nance
Person Months Worked: 4.00 **Funding Support:**
Project Contribution:
National Academy Member: N

Participant Type: Graduate Student (research assistant)
Participant: Paymon Shirazi
Person Months Worked: 5.00 **Funding Support:**
Project Contribution:
National Academy Member: N

Participant Type: Staff Scientist (doctoral level)
Participant: KP Mohanchandra
Person Months Worked: 1.00 **Funding Support:**
Project Contribution:
National Academy Member: N

ARTICLES:

Publication Type: Journal Article Peer Reviewed: Y **Publication Status:** 1-Published
Journal: Applied Physics Letters
Publication Identifier Type: DOI Publication Identifier: 10.1063/1.5093701
Volume: 114 Issue: 14 First Page #: 142403
Date Submitted: Date Published: 4/1/19 9:00PM
Publication Location:
Article Title: Strain control of the Néel vector in Mn-based antiferromagnets
Authors: In Jun Park, Taehwan Lee, Protik Das, Bishwajit Debnath, Greg P. Carman, Roger K. Lake
Keywords: Antiferromagnetic, magnetoelastic
Abstract: Control of the Néel vector in antiferromagnetic (AFM) materials is one of the challenges preventing their use as active device components. Several methods have been investigated such as exchange bias, electric current, and spin injection, but little is known about strain-mediated anisotropy. This study of the AFM L10-type MnX alloys MnIr, MnRh, MnNi, MnPd, and MnPt shows that a small amount of strain effectively rotates the direction of the Néel vector by 90° for all of the materials. For MnIr, MnRh, MnNi, and MnPd, the Néel vector rotates within the basal plane. For MnPt, the Néel vector rotates from out-of-plane to in-plane under tensile strain. The effectiveness of strain control is quantified by a metric of efficiency and by direct calculation of the magnetostriction coefficients. The values of the magnetostriction coefficients are comparable with those from ferromagnetic materials. These results indicate that strain is a mechanism that can be exploited for control of the Néel vect
Distribution Statement: 1-Approved for public release; distribution is unlimited.
Acknowledged Federal Support: **Y**

RPPR Final Report
as of 01-Oct-2021

Publication Type: Journal Article Peer Reviewed: Y **Publication Status:** 1-Published
Journal: Physical Review Applied
Publication Identifier Type: DOI Publication Identifier: https://doi.org/10.1103/PhysRevApplied.9.03
Volume: 9 Issue: 3 First Page #:
Date Submitted: Date Published: 3/1/18 4:00PM
Publication Location:
Article Title: Voltage Control of Antiferromagnetic Phases at Near-Terahertz Frequencies
Authors: Anthony Barra, John Domann, Ki Wook Kim, Greg Carman
Keywords: Antiferromagnetic, magneto elastic
Abstract: Control of the Néel vector in antiferromagnetic (AFM) materials is one of the challenges preventing their use as active device components. Several methods have been investigated such as exchange bias, electric current, and spin injection, but little is known about strain-mediated anisotropy. This study of the AFM L10-type MnX alloys MnIr, MnRh, MnNi, MnPd, and MnPt shows that a small amount of strain effectively rotates the direction of the Néel vector by 90° for all of the materials. For MnIr, MnRh, MnNi, and MnPd, the Néel vector rotates within the basal plane. For MnPt, the Néel vector rotates from out-of-plane to in-plane under tensile strain. The effectiveness of strain control is quantified by a metric of efficiency and by direct calculation of the magnetostriction coefficients. The values of the magnetostriction coefficients are comparable with those from ferromagnetic materials. These results indicate that strain is a mechanism that can be exploited for control of the Néel vect
Distribution Statement: 1-Approved for public release; distribution is unlimited.
Acknowledged Federal Support: **Y**

Publication Type: Journal Article Peer Reviewed: Y **Publication Status:** 2-Awaiting Publicat
Journal: To be submitted Applied Physics Letters
Publication Identifier Type: Other Publication Identifier:
Volume: Issue: First Page #:
Date Submitted: 5/13/20 12:00AM Date Published:
Publication Location:
Article Title: Strain Control of Anisotropy in Polycrystalline NiO
Authors: Barra, A (Barra, Anthony) ; Ross, A (Ross, Andrew) ; Baldrati, L (Baldrati, Lorenzo) ; Lebrun, R (Lebrun,
Keywords: NiO, Antiferromagnetic, measurement
Abstract: As a candidate material for magnetic memory, polycrystalline antiferromagnets offer similar field resilience, THz switching, and lack of stray field as their crystalline counterparts, but with greatly reduced anisotropy and spin dynamics that are not confined to an easy-plane. This makes them ideal for high speed, low power, in-plane switching in magnetic tunnel junctions, provided that suitable memory-read and -write mechanisms can be identified. We report the detection of the antiferromagnetic Néel vector in polycrystalline NiO via spin Hall magnetoresistance (SMR), showing only a 15% amplitude reduction compared to [111] single crystals. The application of 280 ?? of strain leads to an increase in the SMR amplitude by 52% in a constant magnetic field; an equivalent increase to an external field of 3 Tesla, allowing us to quantify the additional anisotropy. We find that the domain structure is highly sensitive to strain, offering an efficient alternative to a magnetic field for alteri
Distribution Statement: 1-Approved for public release; distribution is unlimited.
Acknowledged Federal Support: **Y**

DISSERTATIONS:

Publication Type: Thesis or Dissertation
Institution: University California Los Angeles
Date Received: 13-May-2020 Completion Date: 11/1/19 8:29PM
Title: Magnetic Memory with Antiferromagnets and Multilayers
Authors: Anthony Barra
Acknowledged Federal Support: **Y**

RPPR Final Report
as of 01-Oct-2021

Publication Type: Thesis or Dissertation
Institution: Univeristy of California Los Angeles
Date Received: 13-May-2020 Completion Date: 3/15/19 8:47PM
Title: Novel Magnetoelastic Materials for Multiferroic Applications
Authors: Taehwan Lee
Acknowledged Federal Support: **Y**

Partners

,

I certify that the information in the report is complete and accurate:
Signature: Greg P. Carman
Signature Date: 9/22/21 10:14AM

ARO Final Report Upload

This upload section contains two subsections, i.e. 1) Major Goals and 2) Accomplished

Section 1 – Major Goals

The major aim of this work is to open a new pathway towards THz devices by demonstrating THz magnon-phonon coupling for the first time. To accomplish this, we have targeted antiferromagnets as a material class of interest because their resonance frequencies are much higher than ferromagnets and are often in the THz range. This fact indicates the existence of desirable THz magnon modes, but the level of phonon coupling with these modes is so far unknown. To address this question, our work under this contract seeks to investigate the fundamental physics of antiferromagnets in two main areas: 1) check whether magneto-mechanical coupling at THz is present, since definitive proof is generally lacking, and 2) to prove that strain can be used as a method to control antiferromagnetic states, since this would enable creation or control of THz frequency magnon/phonon excitation.

To prove these two key points, we aim to develop a series of test devices consisting of candidate magnetostrictive antiferromagnetic materials layered into composites with piezoelectric substrates. Using this approach, the composite's strain is tunable with voltage, and can be driven to oscillate at high frequency, thereby allowing observation of both the fundamental strain effects and injection of high frequency phonons. Design of these devices is proceeding following a 3-step process (see Figure 1 below) consisting of 1) sophisticated multiphysical modeling to predict device behavior, 2) fabrication of a device informed by the model results, and 3) testing both of the fundamental mechanical coupling and the device's frequency-dependent magnon-phonon coupling. The goal of this final testing phase is to identify the underlying physics of the mechanical coupling in antiferromagnets, and will require both table-top electrical testing and sophisticated probing of the magnetic properties at national lab beamlines.

To achieve these objectives we focus on two materials, both of which are reported to exhibit three key characteristics, antiferromagnetic order, magnetostriction, and magnetoresistance (magnetoresistance helps to identify the antiferromagnetic state). These two materials are NiO and the 50-50 composition of $L1_0$ ordered alloy FeMn.In addition to these materials, this research covers additional studies conducted by the researchers focusing on ferrimagnetic materials and their related magnetostriction as well as contributions from elemental magnetic moments. While these ferrimagnetic topics are not covered in detail within this report they are part of the published literature that this research supported, i.e. see dissemination section.

Understanding the complex dynamics of antiferromagnets and ferrimagnetics through modeling, fabrication and testing provides a clear path to explore fundamental physics in the context of new and interesting application spaces. Namely, the research conducted here will enable 1) new classes of THz electronic devices, 2) new computational methods verified with experiments, and 3) a fundamental understanding of dynamic THz magnon/phonon interactions. This work aims to launch a major shift towards cheaper and faster electronic devices for future applications.

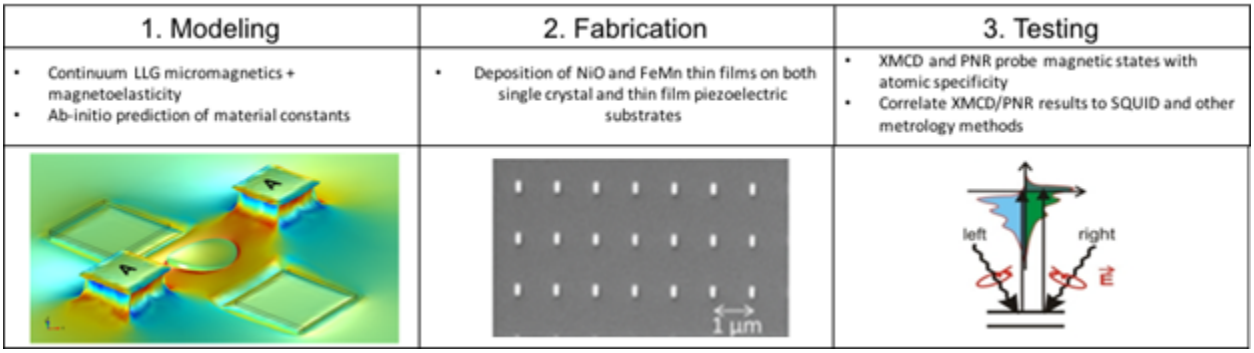

Figure 1 – Three-step plan including fundamental modeling, material fabrication, and testing of strain-mediated voltage control of antiferromagnetic/piezoelectric materials for THz applications.

Section 2 – Accomplished Goals

Over the course of this contract, significant progress was made towards the goal of demonstrating magnetoelectric control of antiferromagnetic states at THz frequencies. Below, the key achievements in each of the three main areas, modeling, fabrication, and testing, are discussed.

1. *Modeling Accomplishments*

The primary goal of the modeling effort was to accurately predict device behavior in magnetostrictive antiferromagnet/piezoelectric composites with THz magnon-phonon coupling. To achieve this goal, both numerical and analytical modeling work was done to simulate the response of magnetostrictive antiferromagnets to strain at THz frequencies, and to identify the dependence of fundamental antiferromagnetic material properties on changes in magnetoelastic energy to help characterize AFM materials and interpret testing results.

A multiphysical finite-element model describing the device-level coupling between mechanical and magnetic states was developed and applied to simulate the behavior of an antiferromagnetic (AFM) bit switching 90˚ in a realistically-sized composite with a piezoelectric substrate (see Figure 2, below). The results in Figure 2a show the components of the magnetization m during the 90˚ rotation, including the net moment (labeled L). The fact that L remains near zero during the rotation means that, in

principle, the speed associated with antiferromagnetic dynamics is much higher than characteristic mechanical speeds, and this has strong implications for how one may design a THz coupled device. Figure 2b shows the coherence of the antiferromagnetic rotation as the strain passes through the antiferromagnet (strain is indicated by the colors inside the element, and the magnetization is indicated by the red and black arrows). These results show that this modeling approach developed by our group can be used to establish a fundamental frequency limitation for realistic device structures while accounting for such complicated effects as the geometry-dependent mechanical impedance matching between the antiferromagnetic and piezoelectric layers [2]. In addition to modeling the time-dependent magnetic response in an AFM/piezoelectric composite, this fully coupled model was used to simulate application-driven devices that rely on high frequency magnon-phonon coupling.

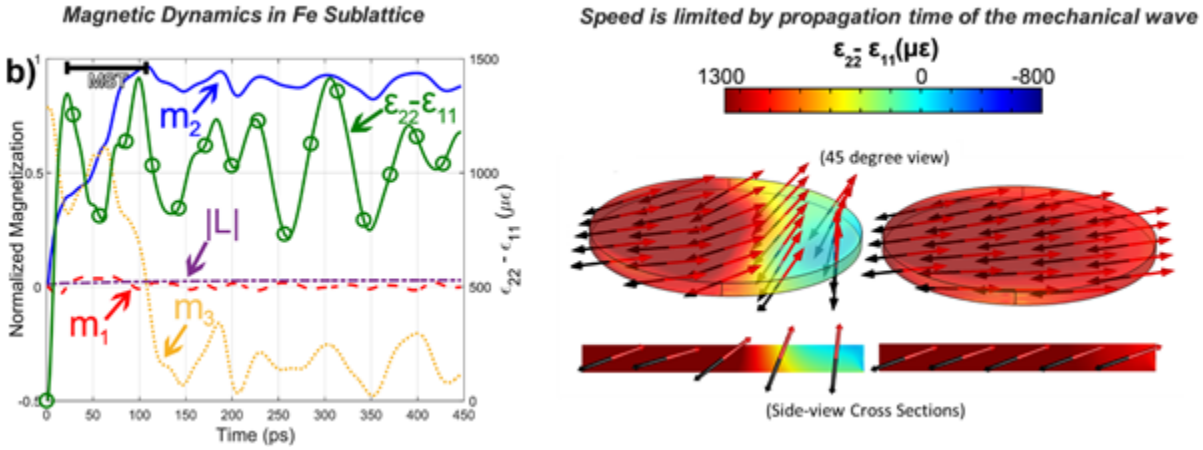

Figure 2 – a) Dynamics of mechanically-induced switching in the Fe sublattice of FeMn subjected to a biaxial strain of 1200 microstrain generated over 50 ps. b) The 80-nm-wide as-modeled FeMn dot is shown mid-switch (left) and post-switch (right). These figures show that the magnetic switching is tightly coupled with the propagation of the exciting acoustic wave, which enters the element from the left.

Neuromorphic computing platforms require programmable synapses to enable brain-like computation. Existing neuromorphic synapses rely on energy intensive electric current to program state changes, and are limited in speed by the ferromagnetic resonance of materials used. Using the above-mentioned finite element model, the response of an antiferromagnetic nanowire to voltage-induced spin waves was simulated. The spin waves drive non-volatile changes in small segments of the antiferromagnetic nanowire's magnetization, stabilized by the material's magnetocrystalline anisotropy. By application of voltage pulses, the nanowire's magnetoresistance can be altered along a spectrum, representing a THz-speed, ultra-low energy option for future neuromorphic computing devices.

Figure 3 illustrates an example of the non-volatile, strain-mediated magnetization changes that can be achieved in the AFM nanowire. Figure 3a plots the magnetization of one of the AFM sublattices and the voltage-induced strain over time. Figure 3b shows snapshots of the magnetization states at times corresponding to the vertical dashed lines in Figure 3a. Initially aligned along the x-axis, the magnetization in 1/3 of the nanowire switches to the z-axis following the first strain pulse (shown at t = 1.5 ns). After the second strain pulse, the magnetization in 2/3 of the nanowire has switched to the z-axis (at t = 3.5 ns). Both of these intermediate states are non-volatile, demonstrating the potential to program a spectrum of resistance states into a magnetoelastic AFM nanowire via strain. This result shows how the finite element AFM model can be utilized to guide and inform AFM device design.

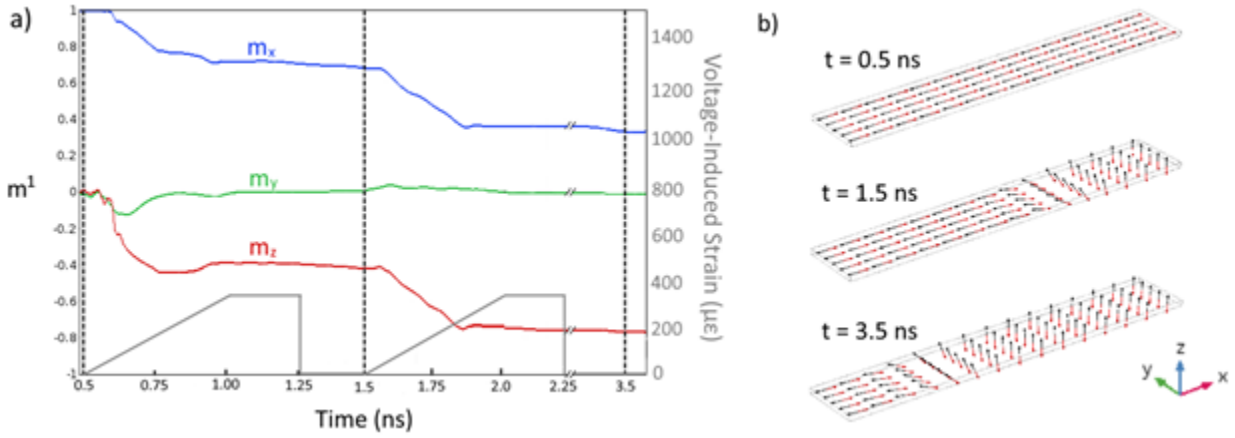

Figure 3 - (a) plots the magnetization of one sublattice and the voltage-induced strain over time. (b) shows snapshots of the magnetization at the points in time marked by vertical dashed lines in (a), illustrating the stable, programmable magnetization states in the FeMn nanowire.

Finally, in addition to simulating the response of antiferromagnetic elements to time-dependent strain, the finite element model was used to support the SMR testbed, discussed below in the testing section (layout shown in Figure 4). The schematic on the left shows the design of the device, with the antiferromagnetic Hall bar in the middle, surrounding Au electrodes for straining, and the axis of applied tension shown with a dotted line. Given this design, modeling was used to simulate the piezoelectric effects of the substrate to estimate the applied strain on the device under each exciting voltage. This simulation allowed for proper placement of the electrodes around the Hall bars, and facilitated interpretation of the experimental results for strained samples since the strain values were known a priori.

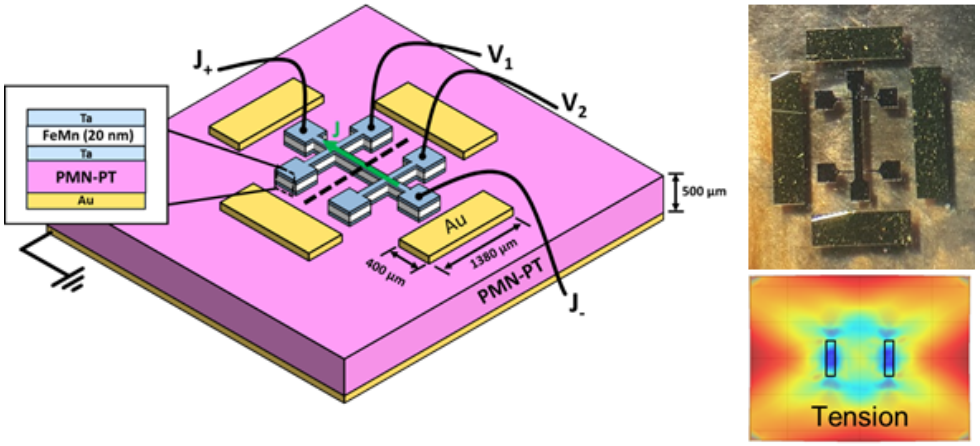

Figure 4 – Left) A diagram of the device for testing strain control of antiferromagnetism is shown. The device utilizes voltage at the Au contacts to strain the Hall bar in the center of the substrate. Top Right) The as-fabricated device is shown. Bottom Right) The model prediction of the strain when 200 V applied across the PMN-PT is shown.

In addition to numerical simulation of magnetostrictive antiferromagnet/piezoelectric composites, analytical modeling was conducted to facilitate material characterization and support device testing. To characterize the saturation magnetostriction in antiferromagnetic alloy FeMn, the contribution to magnetoelastic energy density from applied strains was calculated. For this calculation, we build upon the theory using the magnetoelastic contributions in ferromagnetic materials, in which magnetoelastic energy E_{ME} is given as

$$E_{ME} = \mu_0 M_s \Delta H_c \approx \frac{3}{2}\lambda_s Y \epsilon$$

Where, μ_0 is the permeability of free space, M_s is the saturation magnetization, ΔH_c is the change in the coercive field, λ_s is the saturation magnetostriction, Y is the Young's modulus, and ϵ is the applied strain.This relationship cannot be directly applied to antiferromagnets as M_s and ΔH_c lack meaning for antiferromagnetic materials. However, in-place of the M_s and ΔH_c, the volume susceptibility given as $\chi_v = M/H$

and the antiferromagnetic spin-flop field H_{sf} can be utilized. The maximum volume susceptibility is obtained at the spin-flop field given as $\chi_v = M(H_{sf})/H_{sf}$. In ferromagnets, $M_s$remains constant and the coercive field changes by ΔH_c when strains are applied to these materials. However, in antiferromagnets, both χ_v and H_{sf} change with applied strains and the change in both the volume susceptibility and the spin-flop field must be considered as $\Delta\chi_v$ and ΔH_c, respectively, in the overall magnetoelastic energy. We verify this fact experimentally later in the report. Therefore, the magnetoelastic energy for an antiferromagnet can be written as

$$E_{ME} = \mu_0 \Delta\chi_v \Delta H_{sf} \approx \frac{3}{2}\lambda_s Y \epsilon$$

Using this relationship, we can determine an antiferromagnet's saturation magnetostriction λ_s given its change in volume susceptibility $\Delta\chi_v$ and spin-flop field ΔH_{sf}. This result represents a significant step forward in antiferromagnetic materials characterization, and in the following testing section, this relationship is applied to determine the saturation magnetostriction in our antiferromagnetic FeMn films ($\lambda_s = -141\ ppm$).

Along with conductive antiferromagnet FeMn, a large portion of subsequent testing focuses on insulating antiferromagnet NiO. Spin Hall Magnetoresistance (SMR) represents a key measurement for insulating AFMs, allowing one to experimentally determine the orientation of the Neel vector. To help interpret SMR test results, a model was developed to predict the effect of applied field and strain on SMR signal in polycrystalline NiO. This model represents the antiferromagnetic component of a SMR signal as a function of the Neel vector orientation and applied current direction within each crystallite, represented by:

$$SMR = \rho[1 - \langle (n \cdot e_z \times j_c)^2 \rangle]$$

where ρ is the signal amplitude, e_z represents a unit vector along the film normal, j_c is the SMR current, and $\langle ... \rangle$ indicates the average over all arbitrary orientations of the crystallite axes. The Neel vector orientation within each crystallite is determined by minimization of its energy density, defined by:

$$w_{mag} = \frac{1}{2}H_{\parallel}M_s {n_z}^2 - H_{\perp}M_s({n_x}^2 + {n_y}^2) + \frac{M_s}{2}\left(\frac{H^2}{H_{ex}} + \frac{H_{me}\mu_{piezo}}{\mu_{NiO}}\varepsilon\right)(e_x \cdot n)^2$$

where $H_{\parallel}(H_{\perp})$ is the out-of-plane (in-plane) magnetic anisotropy of the NiO with respect to the magnetic easy-plane, $\frac{M_s}{2}$ is the sublattice magnetization, H_{ex} is the effective

exchange field,H_{me} is the magnetoelastic constant, μ_{NiO} (μ_{piezo}) is the shear modulus of the NiO (PMN-PT substrate), n_j is the j^{th} component of n, and e_x is the unit vector in the X direction. Finally, ε is the strain (linearly proportional to the external stress) applied electrically by the PMN-PT substrate.

Using this model, the dependence of the SMR signal on applied field was determined in the absence of strain for both monocrystalline and polycrystalline samples, and compared to experimental results. Next, the effect of strain on the SMR signal was calculated at applied straining voltages ranging from 0 V to 200 V in steps of 50 V. In the following testing section, these theoretical calculations are compared with experimental results at each applied voltage. The model shows good agreement with experimental results and provides evidence for significant reduction in the SMR saturation field with applied strain as described in the next section. The accuracy of the model supports our understanding of the effect of strain in polycrystalline AFM samples.

2. *Fabrication Accomplishments*

The fabrication work conducted under this contract focused on successfully growing and characterizing both single crystal and amorphous phases of antiferromagnetic alloy FeMn and insulating antiferromagnet NiO. FeMn was deposited via sputter deposition, and NiO grown via electron-beam evaporation. Both materials were deposited on both Si and 500 micron-thick piezoelectric (PMN-PT) substrates.

Using the 6.3.1 beamline at Lawrence Berkeley National Laboratory, both materials were characterized by x-ray circular and linear dichroism (XMCD/XMLD). In these measurements, high energy x-rays with varying polarization states (either circularly or linearly polarized) are used to probe the relative alignment between the x-ray's polarization axis and the magnetic moments in the sample. This allows for determination of the Néel vector in antiferromagnets. Since antiferromagnets have no net moment, this represents a definitive measure of their alignment axis. Such x-ray approaches also allow for atomic specificity when determining the magnetic orientation since the energy of the x-ray can be tuned to the resonant absorption frequencies of the composite elements in an alloy. The goal of these measurements are two-fold, to determine the element-wise contribution to magnetic moment, and to determine the antiferromagnetic to ferromagnetic transition temperatures, both of which are critical to improving our understanding of antiferromagnetic materials for future device applications.

Following the growth of each sample, the crystalline phase of each material was determined through both X-Ray Diffraction (XRD) and Transmission Electron Microscopy's (TEM's) Scanning Electron Area Diffraction (SAED). Then, XMLD and XMCD measurements were used to probe the orientation of each material's magnetic moments. Examples of the XMLD and XMCD measurements on FeMN are shown in Figures 5 and 6. From this data, it was found that the moment of FeMn is dominated by

Mn, indicating that the as-grown samples have some $L1_0$ ordering which may be favorable for magnetostriction. Additionally, by conducting these measurements in the temperature range from 100 to 400K, the antiferromagnetic to ferromagnetic transition temperatures for both NiO and FeMn were found.

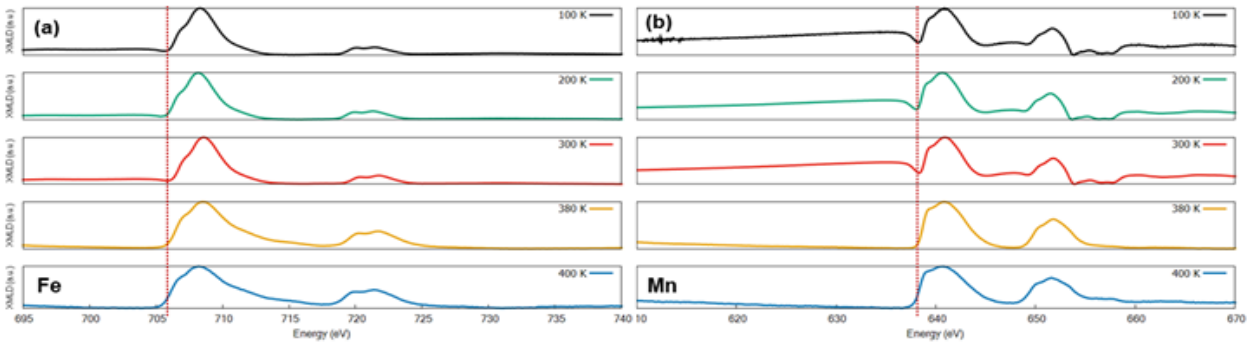

Figure 5 – Temperature dependent XMLD of $L1_0$ FeMn alloy from 100-400 K showing (a) Fe (b) Mn elementwise $L_{2,3}$ edges. Antiferromagnetic to ferromagnetic 2nd order phase transition can be witnessed at 380 K as the Mn L_3 edge (dip) at 638 eV disappers within a strong dichroic absorption. This is an indication that XMLD will no longer provide the $L_{2,3}$ edges at the transition temperature and XMCD a method to probe the ferromagnetic magnetization is required.

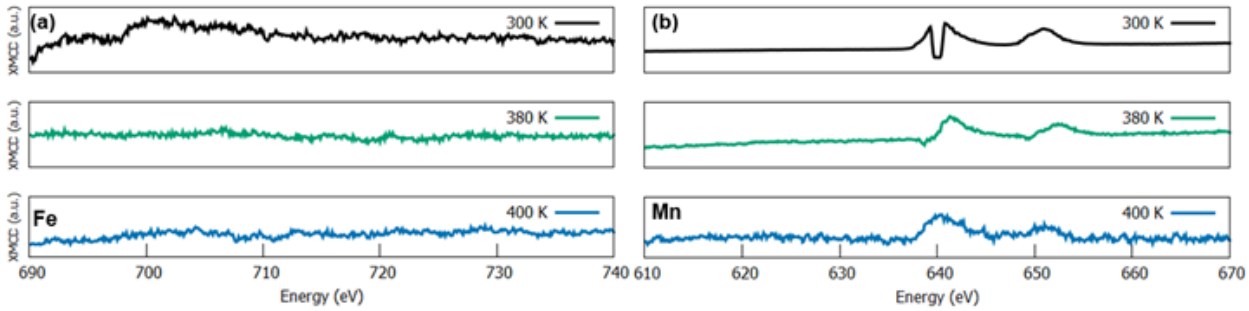

Figure 6 – Temperature dependent XMCD of $L1_0$ FeMn alloy from 100-400 K showing (a) Fe (b) Mn elementwise $L_{2,3}$ edges. Fe does not contribute to either ferromagnetic or antiferromagnetic order in alloy, indicating 2nd order phase transition is due solely to the frustration of the Mn spins. Clear XMCD difference at Mn L_3 edge is witnessed at 380 K, indicating the transition to ferromagnetic order. Mn L_3 edges at 400 K deviate from that at 380 K indicating a weaker ferromagnetic order with increasing temperature.

3. *Testing Accomplishments*

The testing work conducted over the course of this contract focused on measuring the effect of strain on magnetostrictive antiferromagnets FeMn and NiO. This was done via anisotropic magnetoresistance (AMR) and AC-susceptibility measurements on FeMN, and Spin Hall Magnetoresistance measurements (SMR) on NiO.

For the AMR and SMR measurements, FeMn and NiO were deposited on both Si and piezoelectric PMN-PT substrates, and patterned into hall bars (see Figure 4). Current was passed along the length of the Hall bar and resistance was measured along the same length in the usual 4-point-probe resistance measurement configuration. At the same time, an applied field was swept in the range from -11 to +11 T parallel to the hall bar in order to find the resistance as a function of field, and find any potential spin flop field. An example of the SMR of amorphous-NiO/Pt bilayer is shown in Figure 7 below. The parabolic changing resistance with field (a 0.002% change) indicates that it is indeed possible to identify the antiferromagnetic alignment using this approach. Similar results were obtained for FeMn. For both FeMn and NiO, this work represents the first measurement of its kind.

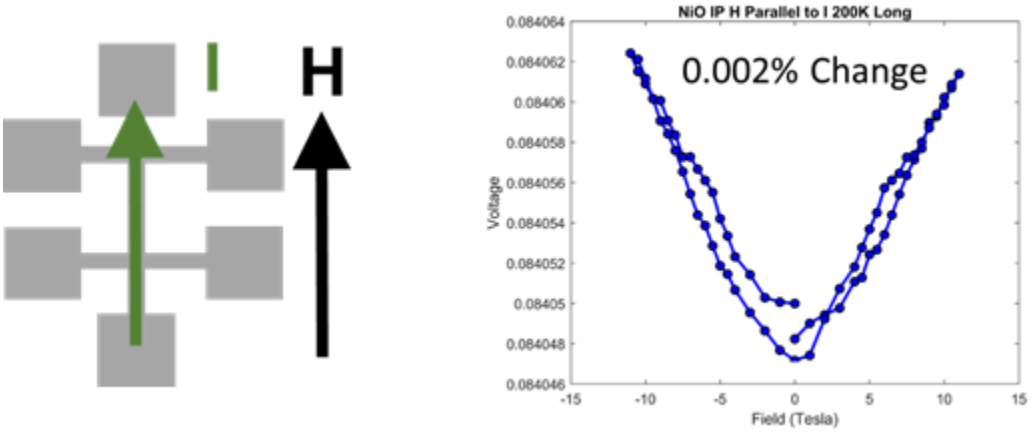

Figure 7 – a) A diagram shows the method of measuring the 4-point resistance, with current running across the top and bottom electrodes, and voltage being measured on two of the side-contacts. b) The longitudinally-measured SMR voltage is plotted against field, showing a characteristic parabolic change, indicating the ability to identify the Néel vector of the NiO by measuring resistance in the neighboring Pt layer.

The above results indicate that magnetic field-dependent spin Hall magnetoresistance (SMR) could be measured in Hall bars of FeMn and NiO. Next, this method was used to demonstrate strain control of antiferromagnetic phases. To do this, SMR was measured in Hall bars with varying magnetic fields and strains applied successively in the range from – 11 T to + 11 T in 1 T steps, and 0 to 300 με in 60 με steps, respectively. The SMR measurement required passing current along the Hall bar's length, and measuring resistance along the same length, using a typical 4-point-probe measurement technique. As a first step, the angle-resolved SMR was checked by

rotating the Hall bar in the 11 T field. When the Hall bar is parallel or perpendicular with the applied field, the SMR in these cases corresponds to the high and low resistance states that one would expect from 90° antiferromagnetic switching.

For NiO in particular, these high and low resistance states were observed to differ by about 0.0007%. Using this as a baseline metric for complete switching, the strain-dependent SMR in NiO was then examined along a single axis, with results shown in Figure 8. To accomplish this, the Hall bar was aligned with the magnetic field and mechanical strain was applied by tuning a voltage from 0 to 200 V in 50 V steps across an underlying PMN-PT substrate, thereby generating strain in the range from 0 and 280 με in 60 με steps. For each strain state, the magnetic field was again swept from -11 T to +11 T while the SMR was measured every 1 T. This experiment showed that 280 με was sufficient to increase the SMR by roughly 40% at every value of applied magnetic field. This means that strain was able to substantially change the susceptibility of the antiferromagnet since more Néel vector rotation was observed for smaller applied fields. Moreover, the sign of the measured susceptibility change matches the expectation that NiO should be negatively magnetostrictive. As biaxial compression was applied to the Hall bar long axis, that axis became magnetically easier. In fact, the observed 40% increase in SMR with strain is similar to that observed under 3 T of applied magnetic field, meaning that the antiferromagnetic ground state is likely dominated by magnetoelastic energy. This insight is the first of its kind and opens a new pathway toward quantifying strain-coupled domain structure changes in NiO. Since there are no alternative experimental techniques, this may prove of significant importance for magnon-phonon coupling in systems at higher frequencies.

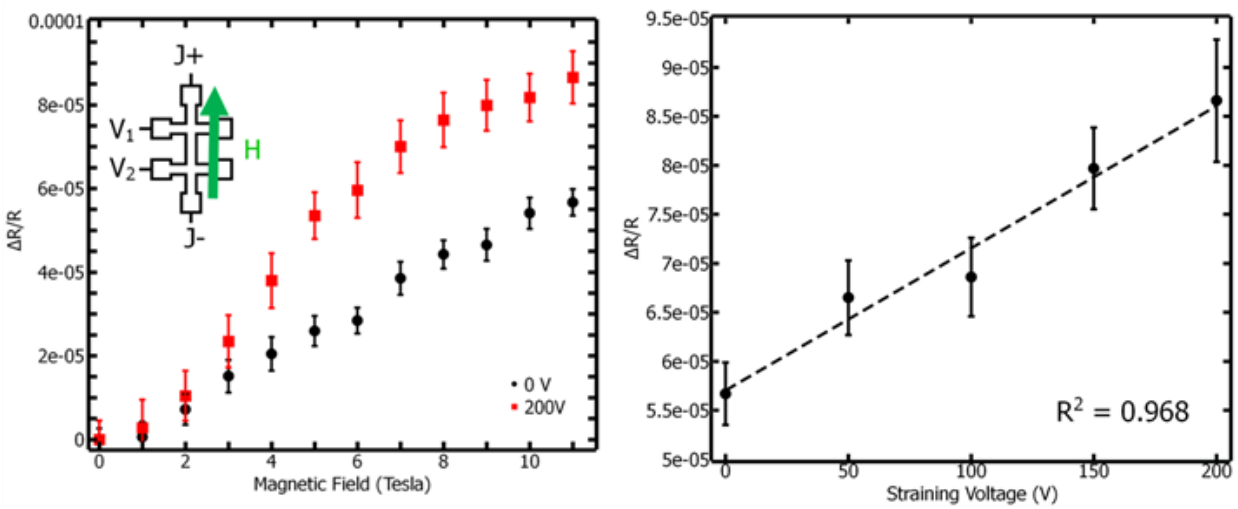

Figure 8 – Left) The uniaxial field-dependent SMR is graphed for two strain conditions, one with 0 V applied to the PMN-PT, and one with 200 V, which corresponds to 280 με. The strain increases SMR by roughly 60% at each magnetic field value. Right) SMR, measured as (R(11 T) – R(0 T))/R(0 T), is plotted for increasing strains, showing a linear change of SMR with strain.

Regarding FeMn, the same angular-dependent SMR measurements that were used as a baseline for 90˚ switching in NiO were used again, with results shown in Figure 9. For FeMn, this measurement produced a sinusoidal SMR as a function of angle, similar to NiO, but the resistance change between the high and low resistance states was on the order of 0.0014%, two times larger than for NiO at 11 T. Using this as a guide, we pioneered a new way to view the magnetoelastic anisotropy changes by attempting to observe the angular-dependent SMR as a function of strain. In this case, the sample was strained along the Hall bar axis and then rotated in a magnetic field while the SMR was measured. We observed that large magnetic fields (> 9 T) created full saturation of the FeMn regardless of strain state, and that excessively small fields created unacceptably small SMR, so these extreme cases were not included. However, between 3 and 9 T, the magnetic field produced measurable SMR, but remained small enough to avoid washing out by the strain effects. In this ideal field range, strain created a phase-lag in the angular SMR when the sample was rotated back and forth in the field. One way to interpret this is that the strain anisotropy canted the Néel vector and that this canting is slightly hysteretic for angular changes in the magnetic field. This effect is shown in Figure 6, below, with the different color sinusoids indicating the forwards (blue) and backwards (black) rotations of the sample.

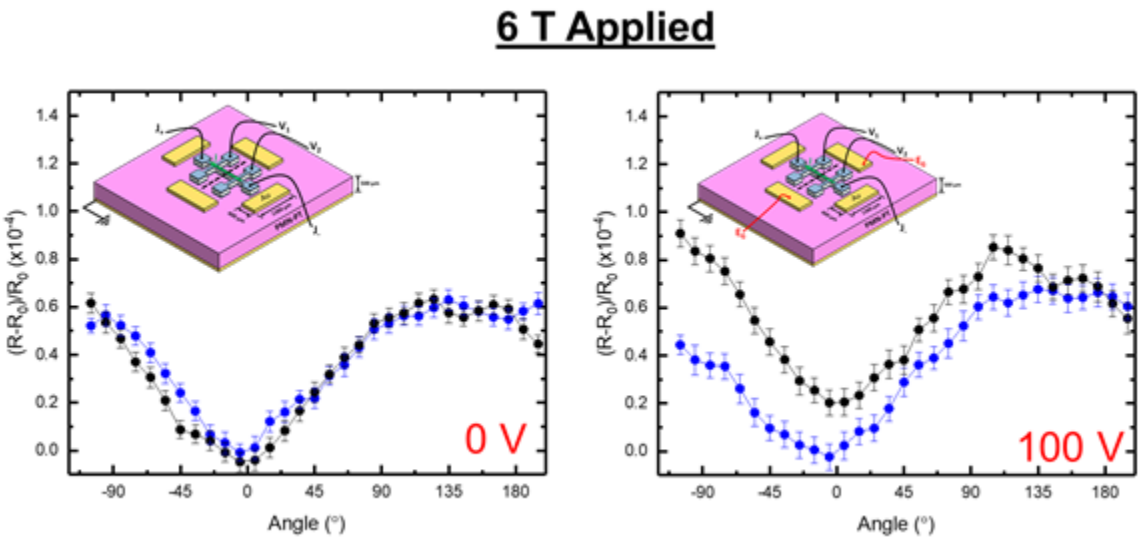

Figure 9 – Left) The uniaxial field-dependent SMR is graphed for two strain conditions, one with 0 V applied to the PMN-PT, and one with 200 V, which corresponds to 280 με. The strain increases SMR by roughly 60% at each magnetic field value. b) SMR, measured as (R(11 T) – R(0 T))/R(0 T), is plotted for increasing strains, showing a linear change of SMR with strain.

By measuring SMR as a function of applied strain, direct evidence of strain controllable antiferromagnetic states was obtained.The next testing phase focused on clarifying the effect of polycrystallinity on SMR signal in NiO hall bars under the influence of voltage-induced strain. A heterostructure of polycrystalline NiO and Pt was

deposited via electron-beam evaporation and patterned into a hall bar on top of a PMN-PT substrate. SMR measurements were conducted by measuring voltage across the hall bar as the SMR current was applied, as shown in Figure 10a.

Initial measurements focused on confirming that SMR can measure the average Neel vector orientation in polycrystalline samples. Figure 10b shows the angle dependent SMR ratio obtained at two applied fields (3 T and 11 T), confirming the sensitivity of SMR to the Neel vector orientation in our sample. Next, with the external field and SMR current aligned colinearly such that maximum SMR is produced, the field dependence of the SMR signal was obtained for applied fields ranging from 0 T to 11 T in steps of 1 T, and applied straining voltages ranging from 0 V to 200 V in steps of 50 V. These results are presented in Figures 11a-11e. Figure 11a compares measured SMR data to that predicted by the model mentioned above for both epitaxial (dashed line) and polycrystalline (blue line) NiO, showing good agreement between the model for polycrystalline samples and experimental results.

At each of the subsequent applied voltages (Figures 11b-11e), the experimental data closely matches that predicted by the model. Figure 11f plots the voltage dependence of the spin-flop field, extracted from the field dependent SMR results. This plot shows that as the straining voltage is increased, the spin-flop field is reduced. This result is evidence that the application of tensile strain perpendicular to the applied field assists in aligning the AFM spins. Extrapolating from this data, the spin-flop field drops to 0 T for 275 V straining voltage, indicating that at this voltage, a spin-flop transition could occur via strain in the absence of applied magnetic field. These results illustrate that even in polycrystalline samples, voltage-induced strain can effectively manipulate AFM spin states. This work is now published in Applied Physics Letters [3].

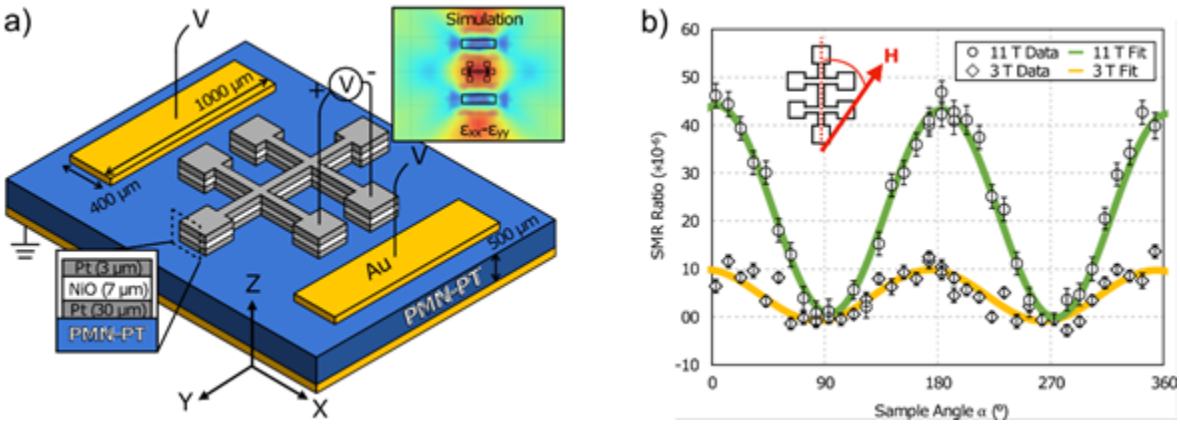

Figure 10. - a) A schematic of the NiO hall bar structure and voltage probe placement. b) Angle dependent SMR signal for 3 T and 11 T applied field.

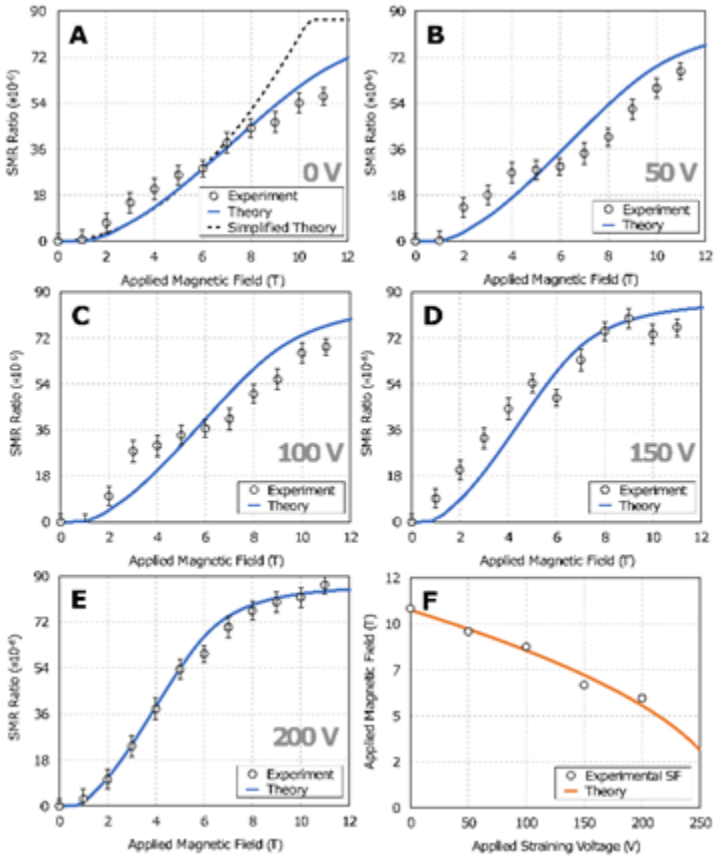

Figure 11. - a) Comparison of field dependent SMR ratio data to theoretical results for both a monocrystalline and polycrystalline model. b) – e) Experimental and theoretical field dependent SMR ratios for increasing straining voltages, from 50 V to 200 V. f) Spin-flop fields as a function of applied straining voltage.

To quantify the strength of magnetostrictive coupling in FeMn, the antiferromagnetic order, susceptibility, and spin flop field of FeMn films with varying process parameters were determined. Variation of the argon working pressure during DC sputtering of FeMn results in films with tensile and compressive stresses with negligible effect on composition, as shown in Figure 12(a). In Figure 12(b), the effect of

argon working pressure, and hence, the residual stress in the film, on magnetic order is shown. For pressures of 5, 10, and 15 mTorr, the films show paramagnetic, mixed paramagnetic-antiferromagnetic, and antiferromagnetic response, respectively. The inset in Figure 12(b) zooms in to the low magnetic field-magnetization behavior and shows a clear paramagnetic response for the 5 mTorr film, and clear antiferromagnetic response for the 10 and 15 mTorr films. Following these measurements, x-ray diffraction measurements were conducted showing only α-phase FeMn for the 5mTorr sample, but a mixture of α and γ-phase FeMn in the 10 and 15 mTorr samples. These results demonstrate that the magnetic properties of sputtered FeMn films can be controlled via process parameters (i.e. argon working pressure).

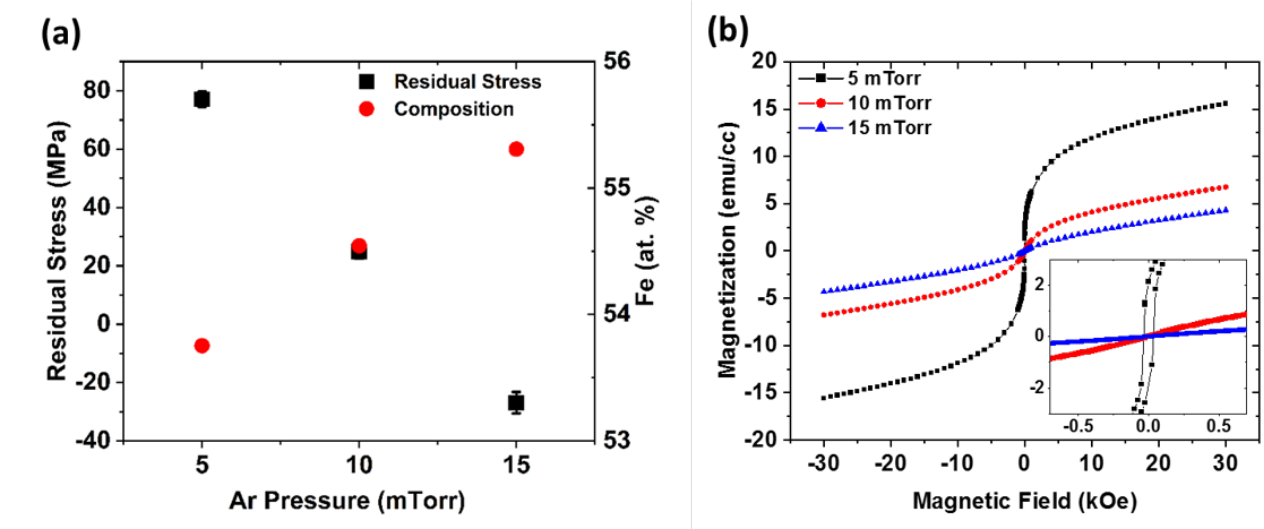

Figure 12 – a) Residual Stress (left-ordinate axis) and Fe composition (right-ordinate axis) versus the Argon working pressure for magnetron sputtered FeMn thin films b) Magnetization curves for three for three magnetron sputtered FeMn thin films at different Argon working pressures

The two FeMn samples prepared at 10 and 15 mTorr were subsequently studied to determine their spin-flop field (H_{sf}) using AC-susceptibility measurements in a SQUID magnetometer. The purpose of this test was to determine the orientation of the Neel vector (i.e. in-plane or out-of-plane) and to demonstrate the dependence of Neel vector orientation on residual film stress. In Figure 13, in-plane and out-of-plane magnetization curves (left-ordinate axis) and AC-susceptibility measurements (right-ordinate axis) are shown for the (a) 10 mTorr and (b) 15 mTorr FeMn samples. The variation in argon working pressure produced a difference in residual stress between these films of 52 MPa. The 10 mTorr sample (Figure 13a) shows a Neel vector that lies in-plane (i.e. red susceptibility curve), whereas for the 15 mTorr film (Figure 13b) the Neel vector lies out-of-plane (i.e. black susceptibility curve). This demonstrates that a 52 MPa difference in residual stress can significantly affect Neel vector orientation.

The measured difference in spin-flop field (γ-H_{sf}) between the 10 mTorr and 15 mTorr films (shown as insets in Figures 13a and b) was roughly 10 kOe (32 kOe for 10 mTorr film, 42 kOe for 15 mTorr film), owing to variations in the total anisotropic energy landscape due to residual stress. This serves as additional evidence that residual stress in antiferromagnetic thin-films may induce an in-plane to out-of-plane reorientation of the Neel vector. Using this experimental data and the stress difference of 52 MPa, along with the results of the above-mentioned analytical model, we estimate that FeMn possesses negative magnetostriction with a saturation magnetostriction value of $\lambda_s = -141\ ppm$.

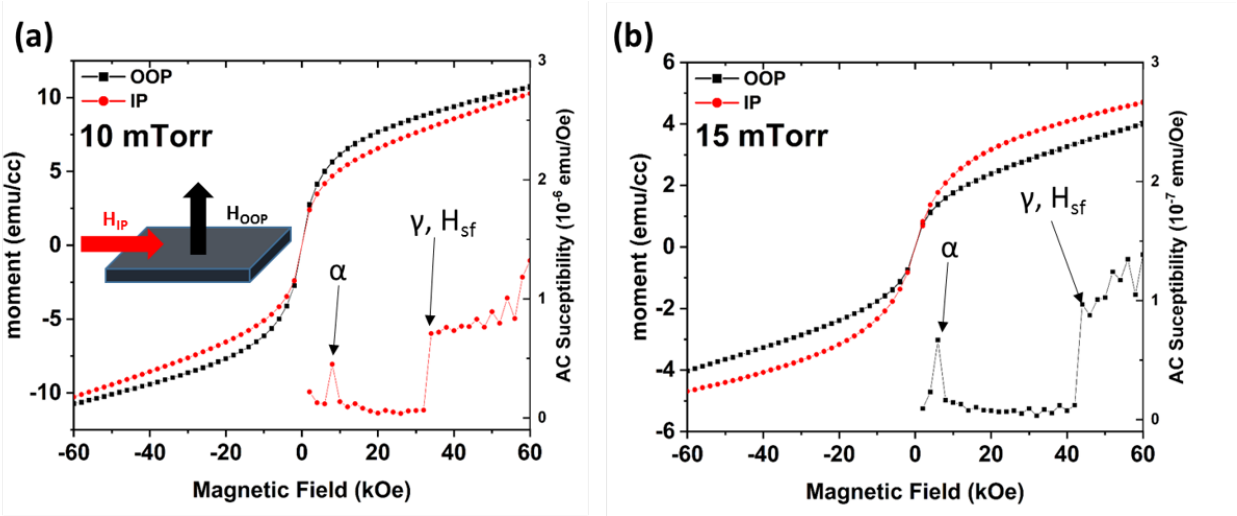

Figure 13 – In-plane (IP) and out-of-plane (OOP) magnetization curves (left-ordinate axis) and AC-susceptibility (right-ordinate axis) for FeMn thin-films prepared at an Argon working pressure of a) 10 mTorr and b) 15 mTorr